Physics and Imaging in Radiation Oncology 7 (2018) 58–64

Contents lists available at ScienceDirect

Physics and Imaging in Radiation Oncology

journal homepage: www.elsevier.com/locate/phro

Original Research Article

Feasibility of magnetic resonance imaging-only rectum radiotherapy with a commercial synthetic computed tomography generation solution

Matteo Maspero[a,b,*], Marcus D. Tyyger[c,a], Rob H.N. Tijssen[a], Peter R. Seevinck[d,b], Martijn P.W. Intven[a], Cornelis A.T. van den Berg[a,b]

[a] Department of Radiotherapy, Universitair Medisch Centrum Utrecht, The Netherlands
[b] Center for Image Sciences, Universitair Medisch Centrum Utrecht, The Netherlands
[c] Leeds Teaching Hospital, Department of Medical Physics and Engineering, Leeds, United Kingdom
[d] Image Science Institute, Universitair Medisch Centrum Utrecht, The Netherlands

ARTICLE INFO

Keywords:
MRI
MR
CT
Medical imaging
Dose calculation
MR-only radiotherapy
Position verification
Image-guided radiotherapy
IGRT

ABSTRACT

Background and purpose: Synthetic computed tomography (sCT) images enable magnetic resonance (MR)-based dose calculations. This work investigated whether a commercially available sCT generation solution was suitable for accurate dose calculations and position verification on patients with rectal cancer.

Material and methods: For twenty rectal cancer patients computed tomography (CT) images were rigidly registered to sCT images. Clinical volumetric modulated arc therapy plans were recalculated on registered CT and sCT images. Dose deviations were determined through gamma and voxelwise analysis. The impact on position verification was investigated by identifying differences in translations and rotation between cone-beam CT (CBCT) to CT and CBCT to sCT registrations.

Results: Across twenty patients, within a threshold of 90% of the prescription dose, a gamma analysis (2%, 2 mm) mean pass rate of 95.2 ± 4.0% (± 1σ) and mean dose deviation of −0.3 ± 0.2% of prescription dose were obtained. The mean difference of translations and rotations over ten patients (76 CBCTs) was < 1 mm and < 0.5° in all directions. In the sole posterior-anterior direction a mean systematic shift of 0.7 ± 0.6 mm was found.

Conclusions: Accurate MR-based dose calculations using a commercial sCT generation method were clinically feasible for treatment of rectal cancer patients. The accuracy of position verification was clinically acceptable. However, before clinical implementation future investigations will be performed to determine the origin of the systematic shift.

1. Introduction

Radiotherapy is an effective treatment modality for rectal cancer patients [1]. In combination with chemotherapy, neoadjuvant radiotherapy prescribing approximately 50 Gy in 1.8–2.0 Gy fractions (long-course radiotherapy) is considered the standard of care for locally advanced rectal cancers when followed by total mesorectal excision (TME) surgery [2]. For non-locally advanced stage III rectal cancer, short-course radiotherapy consisting of neoadjuvant therapy (5 × 5.0 Gy) followed by immediate TME surgery is the standard of care. This short-course radiotherapy scheme showed a reduction in the risk of local recurrence compared to TME surgery alone [3].

For the planning of radiotherapy, magnetic resonance imaging (MRI) demonstrated its superior soft tissue contrast compared to computed tomography (CT) [4]. In the case of rectal cancer, MRI showed prognostic power for staging capabilities [5,6] and reducing the radiotherapy volumes by approximately 20% and inter-observer variability with respect to CT-based delineations [7,8].

Despite these benefits, radiotherapy cannot be planned on MR images alone, as they do not provide the tissue electron density information required for dose calculations [9]. This lead to the adoption of hybrid MRI/CT pathways, which required multimodality image registration [10]. However, such a workflow is susceptible to systematic and random spatial uncertainties originating from registration errors [11,12]. MR-only workflows have been proposed [11] to overcome these uncertainties, as well as, to offer practical and logistical advantages, by reducing: the overall treatment cost [13], workload [14], and patient exposure to ionising radiation [10]. To clinically introduce MR-only

* Corresponding author at: Department of Radiotherapy, Universitair Medisch Centrum Utrecht, Heidelberglaan 1003584 CX, Utrecht, The Netherlands.
E-mail addresses: m.maspero@umcutrecht.nl, matteo.maspero.it@gmail.com (M. Maspero).

https://doi.org/10.1016/j.phro.2018.09.002
Received 17 May 2018; Received in revised form 15 September 2018; Accepted 20 September 2018

radiotherapy, MR-based dose calculations and position verification either based on MRI or MRI-derived images should be enabled and evaluated.

Recently, MR-only simulation has been proposed including the generation of synthetic-CT (sCT) images [15] to enable dose calculations and position verification. Investigations into sCT generation mostly focused on brain and prostate cancer patients [16,17], with vendors recently providing certified solutions for prostate cancer radiotherapy [18–20]. Only two publications investigated the feasibility of MR-only radiotherapy calculations for rectal cancer patients [21,22]. These two contributions focused solely on the dosimetric accuracy of MR-based dose calculation without investigating the use of sCT as a reference for position verification.

This study investigated whether one of the commercial solutions certified for prostate cancer patients can also be employed for rectal cancer patients. Notably, this study evaluated the use of sCT images for cone-beam CT (CBCT)-based position verification.

2. Materials and methods

2.1. Patient data collection

This study was conducted on fifteen male and five female rectal cancer patients that were free from hip implants and who underwent external beam radiotherapy. All patients had previously provided written informed consent regarding the use of their images, in accordance with the Medical Ethical Committee requirements. The patients were diagnosed with intermediate, and high-risk rectal cancer staged T1c-T4. Their mean age was 60 ± 10 years (± 1σ; range 38–75 years), and their mean body mass index was on average 27 kg/m^2 (range 23–39 kg/m^2). The patients were treated for neoadjuvant therapy; Three fractionation regimes were adopted: short course treatment delivering 5 × 5.0 Gy (3), and long-course treatment 25 × 2.0 Gy without (14), and with (3) an integrated boost on extra-mesorectal pathological nodes of 25 × 2.4 Gy. Nineteen patients were irradiated with volumetric modulated arc therapy (VMAT) consisting of two coplanar arcs of 10 MV between 50° and 310°. One patient was irradiated with a single 360° VMAT arc. All plan were clinically optimised according to dose prescription to organs reported in the Dutch guidelineshttp://www.oncoline.nl/colorectaalcarcinoom.

Patients' simulations were performed on both CT and MRI between October 2015 and May 2017 at the University Medical Center Utrecht. For all patients, 3T MRI (Ingenia MR-RT, v 5.1.7, Philips Healthcare, The Netherlands) was acquired within 3 h of CT (Brilliance Big Bore, Philips Healthcare, Ohio, USA), with a mean time of 73 min between the two imaging sessions. All patients were asked to drink 200–300 ml of water one hour before the acquisition after emptying their bladder. Patients were positioned on the vendor-provided flat table and using a knee support cushion (lower extremity positioning system, without adjustable FeetSupport, MacroMedics BV, The Netherlands). To facilitate treatment positioning, patients were tattooed at the CT and positioned at the MRI with the aid of a laser system (Dorado3, LAP GmbH Laser Applikationen, Germany).

CT scans were performed with the following parameters: 120 kV, 923 ms exposure time, 121–183 mA tube current, 512 × 512 pixels in-plane matrix, and 3 mm slice thickness. In-plane resolution varied depending on the field of view (FOV) used, with an average pixel size of 1 × 1 mm^2 and maximum size of 1.2 × 1.2 mm^2. The typical size of the FOV was 50 × 50 × 30 cm^3, expressed in terms of anterior-posterior, right-left and superior-inferior directions.

MR images were acquired using anterior and posterior phased array coils (dS Torso and Posterior coils, 28 channels, Philips Healthcare, The Netherlands). To avoid skin contour deformation, two in-house-built bridges supported the anterior coil. For the generation of MR-based sCT images, a dual echo three-dimensional (3D) Cartesian radio-frequency spoiled gradient-recalled echo sequence was acquired with the imaging parameters expressed in Table 1.

Table 1
Image parameters of the sequences used for the sCT generation. The terms FOV refers to the field of view, while AP to anterior-posterior.

Imaging parameters	Value
$TE_1/(TE_2)/TR$ [ms]	1.2/2.5/3.9
Flip Angle [°]	10
FOV* [cm^3]	55 × 55 × 30
Acquisition Matrix*	324 × 324 × 120
Reconstruction Matrix*	512 × 512 × 120
Reconstructed Voxel* [mm^3]	1 × 1 × 2
Bandwidth [Hz/px]	1072
Readout direction	AP
Geometry correction	3D
Acquisition time	2 min 17 s

* expressed in terms of anterior-posterior, right-left and superior-inferior directions.

A Dixon [23] reconstruction [24] was performed obtaining in-phase, fat, and water images. Using the acquired MR images, sCTs were generated with a proprietary solution tailored to prostate patients called "Magnetic Resonance for Calculating ATtenuation" (MRCAT, Ingenia MR-RT 5.1.7, rev. 257, Philips Healthcare, Finland). The imaging parameters were locked by the vendor as part of the proprietary solution. The sCT generation occurred directly at the scanner as an integrated reconstruction and employed a model of bone resulting in five bulk-density assigned sCT images. The transverse plane of a CT (a) and sCT (b) for one example patient are shown in Fig. 1.

Delineations were drawn by a radiation oncologist, with target delineations on the MRI composed of T2-weighted turbo spin echo and diffusion-weighted imaging as described in [25] and organs at risk (OARs) delineations on CT. To delineate the structures, MRI was rigidly registered to CT using an in-house developed software [26].

Patients underwent image-guided radiotherapy (IGRT) with pre-treatment position verification on a kV CBCT system integrated into the gantry of linear accelerators (XVI, v 5.0.2b72 Elekta AB, Sweden) with the following imaging parameters: 120 kV, 1175 mAs, 41 × 41 × 26 cm^3 FOV, 1 × 1 × 1 mm^3 voxel size, detector position was medium, filter F1, counter-clock rotation from −180° to 180° with 0.25 rps gantry speed and 5.5 fps frame rate. Different correction protocols were followed according to the fractionation regime: for five-fraction short-course radiotherapy online correction was performed every fraction, while for 25-fraction long-course radiotherapy the extended non-action level (eNAL) protocol [27] was performed. Set-up errors according to the eNAL protocol were estimated in the first three fractions, followed by imaging every five fractions. All patients expected to undergo five to seven CBCT; for a few patients, the imaging frequency was increased, e.g. based on the amount of inter-fraction motion observed. Set-up corrections were estimated by registering CBCT to the planning CT based on bony anatomy via chamfer matching [28] with six degrees of freedom (DoF) (translation and rotation), which is the local clinical protocol. Registrations with three DoF (translation only) were also performed for completeness. Registrations were estimated within a clipbox including bony pelvic anatomy whilst excluding femoral heads and trochanter minor where possible. The centre of the rotation was assigned as the centre of the planning treatment volume (PTV) or the gross tumour volume (GTV).

2.2. sCT evaluation

The clinical suitability of utilising MRCAT as an sCT generation technique for rectal cancer patients was evaluated. CT images were rigidly registered and resampled to the voxel size of sCT images with Elastix v4.7 (Klein et al. 2010) using mutual information and trilinear interpolation as previously reported [19]. The registered CT images were visually inspected. In the following, we use the term CT_{reg} to refer to registered CT images.

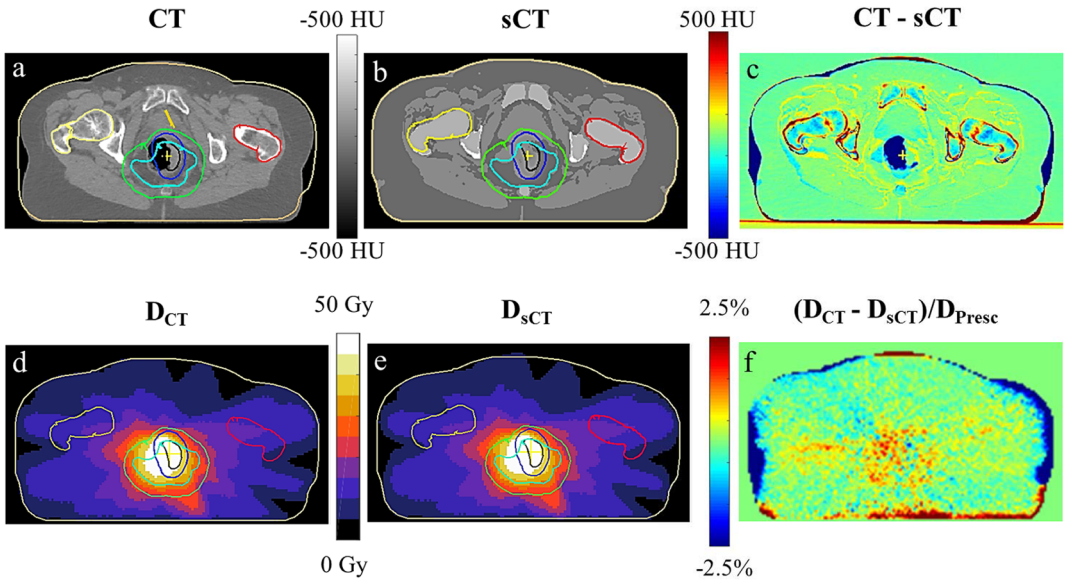

Fig. 1. *Top row*: CT_{reg} (a, left), sCT (b, middle) and CT_{reg} minus CT (c, right) for a female patient staged cT4N1, 66 years old, 74 kg, 167 cm, BMI = 26.5 treated with 25 × 2.0 Gy with integrated boost. *Bottom row*: Doses calculated on CT_{reg} (d, left) and sCT (e, middle), while on the right (f) the dose difference (CT_{reg}-sCT) is presented as the percentage of the prescribed dose (50 Gy). The delineation of the external body contour on sCT (orange) and of femurs (yellow and red), CTV of the primary tumour (light blue), PTV of the primary tumour (green), PTV of the boost (blue) and GTV of the boost (black) on CT_{reg} are visible. (For interpretation of the references to colour in this figure legend, the reader is referred to the web version of this article.)

2.2.1. Image comparison

Image evaluation was performed by calculating the mean absolute error (MAE) and mean error (ME) (± 1σ) with respect to CT_{reg} within the body contour intersection of sCT and CT_{reg}. The body contours were automatically obtained by thresholding CT_{reg} and sCT images at −200 HU. Fig. 1(c) shows CT_{reg} minus sCT for one example patient.

2.2.2. Dose comparison

Before planning, the clinical delineations were propagated to sCT and CT_{reg} images except for the body contours, which were automatically generated. Clinical plans were recalculated on sCT and CT_{reg} images in Monaco (v 5.11.02, Elekta AB, Sweden) using the Monte Carlo photon algorithm on a grid of 3 × 3 × 3 mm^3 with 1% statistical uncertainty. Gaseous regions within CT_{reg} had their electron densities (ED) set to water, following the UMC Utrecht clinical pathway. No gaseous regions were created during sCT production; therefore no ED filling was required. To ensure that consistent isocenters were used on sCT and CT_{reg} images, isocenters were assigned as the centre of the PTV.

Dose distributions were analysed through dose differences ($\frac{CT - sCT}{prescribeddose}$ and $\frac{CT - sCT}{CT}$) and 3D gamma analysis at 3%,3 mm and 2%,2 mm [29] relative to dose on CT_{reg} within dose threshold regions of 90%, 50%, and 10% prescription dose and in the body contour intersection after a 15 mm cropping to take account of dose build-up. For gamma analysis a search radius of 5 mm, and a dose grid of 2 × 2 × 2 mm^3 was used with the dose on CT as reference. Analysis of dose-volume histogram (DVH) points was performed to verify target (CTV, PTV) dose coverage and adherence to OARs constraints considering the differences between dose points (D_{98}, D_{50}, D_2, V_{95}, V_{75}) on the CT and sCT plans for CTV, PTV and bladder.

2.2.3. Position verification

The CBCTs of ten patients (three female, seven male) could be retrieved and were rigidly registered to sCT, and CT_{reg} in XVI, the clinical software used for position verification. Registrations were automatically performed based on bone matching utilising chamfer matching implemented in XVI [28] under the supervision of an operator. The operator manually initialised the registration in case of visible misregistration. Translations and rotations, if calculated, were reported from three and six DoF bony match registration within the clipbox which was set following the local clinical guidelines. The correction reference point (rotation point) chosen for the six DoF registration was the centre of the gross tumour volume GTV or PTV both for CT and sCT, following the previous clinical choice. The difference in translation (ΔT) and rotation (ΔR) between CBCT to CT and CBCT to sCT was calculated. The mean ± 1 standard deviation (σ), and range of these differences in right-left (RL), inferior-superior (IS), posterior-anterior (PA) directions were reported. Two one-sided tests were performed to verify equivalence with a range of (−1 mm; 1 mm) for the mean ΔT and ΔR of the patients at a 95% confidence interval [30].

3. Results

3.1. Image comparison

Across twenty patients, the average MAE and ME in the body contour intersection were 52 ± 3 HU (± 1σ, range = 47–59 HU) and 8 ± 6 HU (range = −8-15 HU), respectively. Fig. 1 (bottom row) shows the doses on CT (d), sCT (e) and their percentage difference (f) for an example patient. It can be noticed in panel (c) that the largest differences between CT and sCT can be found at the body contours, bone/soft tissue interface and in the rectum due to the presence of air pockets that were not represented in the sCT images.

3.2. Dose comparison

A mean dose deviation of −0.1 ± 0.1% and −0.5 ± 0.3% (± 1σ) of the prescription dose and relative to CT were obtained using a threshold of 10% (D>10%) of the prescription dose. Within this volume, a gamma (2%, 2 mm) pass rates of 94.7 ± 1.7% was obtained.

On average, sCT images resulted in a higher dose to the target (in the high dose region, D>90%), with a mean increase of 0.3% over the prescribed dose. In the worst case, the mean dose difference was 0.6%. The mean gamma pass rates using the 3%,3 mm and 2%,2 mm criteria were > 96 and 85%, respectively, for all volumes of interest, as reported in Table 2.

Table 2
Statistics of the dose comparison on twenty rectal cancer patients. Mean dose difference relative to the prescription dose and gamma pass rate of the average dose difference calculated on a threshold of 10%, 50%, 90% of the prescription dose and the body contour intersection between CT and sCT images (Body). The values are reported in percentage in terms of mean (± 1σ) and range [min; max].

Volume of interest	Dose Difference $\frac{CT-sCT}{D_{Prescr}}$ [%]	Dose Difference $\frac{CT-sCT}{CT}$ [%]	Pass Rate $\gamma_{3\%,3mm}$ [%]	Pass Rate $\gamma_{2\%,2mm}$ [%]
D>10%	−0.1 ± 0.1 [−0.3;0.1]	−0.5 ± 0.3 [−1.5;0.1]	98.1 ± 0.9 [96.1;99.8]	94.7 ± 1.7 [91.2;98.1]
D>50%	−0.2 ± 0.2 [−0.5;0.3]	−0.6 ± 0.2 [−1.6;0.3]	99.0 ± 0.9 [97.1;100]	95.9 ± 2.7 [89.3;99.0]
D>90%	−0.3 ± 0.2 [−0.6;0.4]	−0.5 ± 0.2 [−1.3;0.4]	99.5 ± 0.7 [97.2;100]	95.2 ± 4.0 [85.4;99.8]
Body	0.1 ± 0.1 [−0.2;0.1]	−0.4 ± 0.4 [−1.3;0.1]	98.6 ± 0.6 [96.6;99.7]	96.1 ± 1.3 [92.5;98.2]

As part of the Supplementary material, which is online available at ADD_URL (to be done by the journal), we reported the dose differences on a patient basis as well as geometrical evaluations in terms of beam depth and radiological beam path.

All DVH points for target (PTV, CTV) and bladder differed < 0.5% (mean) and at maximum 2.5% on sCT with respect to CT, as also presented in Fig. 2.

3.3. Position verification

A total of 76 CBCT scans were used for registration, ranging from five to twelve CBCTs per patient over the ten patients considered. For all patients automatic registration was used and six CBCT registrations required operator intervention to facilitate automatic registration. Boxplots of differences in translation (ΔT, in mm) and rotation (ΔR, in °) between set-up corrections obtained registering CBCT to sCT minus CBCT to CT_{reg} is presented in Fig. 3. The mean differences were < 0.5 mm and < 0.5 ° in all the direction, except PA, where a systematic difference < 1 mm was found, as reported in Table 3. For all patients, using three and six DoF registrations, no translations or rotations were >±2 mm and 1.2°, respectively. The PA direction resulted in shifts that were not equivalent and statistically different according to the one-sided tests at 95% confidence interval within ± 1 mm both for three and six DoF registration. This was interpreted as a systematic deviation impacting this direction.

4. Discussion

We demonstrated the clinical feasibility of employing a commercial prostate cancer sCT generation method for patients with rectal cancer, with dose differences of 0.3% achieved compared to CT-based calculations. This result indicated that the adopted commercial prostate sCT generation method could facilitate the introduction of MR-only rectal radiotherapy without alteration.

The dose deviations obtained in this study are in line with previously published studies on rectal cancer patients [21,22], which reported dose differences within 1.5% and to other studies in the pelvic area reporting dose differences within 2% [31,15,16]. As highlighted in the Supplementary material, the observed dose differences may be related to smaller body contour on sCT with respect to CT images. However, further studies are necessary to verify the cause of these differences. Focusing on the studies published on rectal cancer patients, Kempainnen et al. obtained a median gamma pass rate (2%,2 mm) of 99.3% excluding points with dose < 30% of the maximum dose [21] and Wang et al. a median above 99% excluding points with dose < 10% of the maximum dose [22]. Compared to our investigation, they both obtained higher gamma pass rates. However, in both the studies, body contour matching between CT and sCT was performed resulting in a higher pass rate compared to our result.

Dose deviations should be interpreted in the context of the clinically acceptable uncertainty in radiation therapy. When considering the complete radiotherapy pathway, including uncertainties in beam calibration, relative dosimetry, dose calculations, and dose delivery, the International Commission on Radiation Protection estimated uncertainty of 5% in a clinical set-up [32,33]. The dosimetric deviation of an MR-based dose calculation (assuming CT to be the ground truth) of less than 0.5% only makes up for a small fraction of the total uncertainty [18].

It is of particular interest to observe whether dose differences were larger for females with respect to males, considering that the commercial solution evaluated in this study was initially released only for prostate cancer patients. In our dataset, five of twenty patients were female and, as reported in the Supplementary material, no evident dose differences were found on this population. However, the female population is small and further investigations are required to ensure the safe use of sCT on this patient group.

Set-up corrections during an IGRT treatment aim at ensuring that a patient may assume an identical posture and position between an irradiation and simulation sessions [34]. An institute that introduces an MR-only pathway needs to assess whether set-up corrections during IGRT can be accurately performed solely utilising sCT images or MR-based surrogates as references.

In this study, we found that the use of sCT did not impact set-up corrections for RL and IS directions. However, in the PA directions, we observed a systematic difference < 1 mm. As for the dose evaluation,

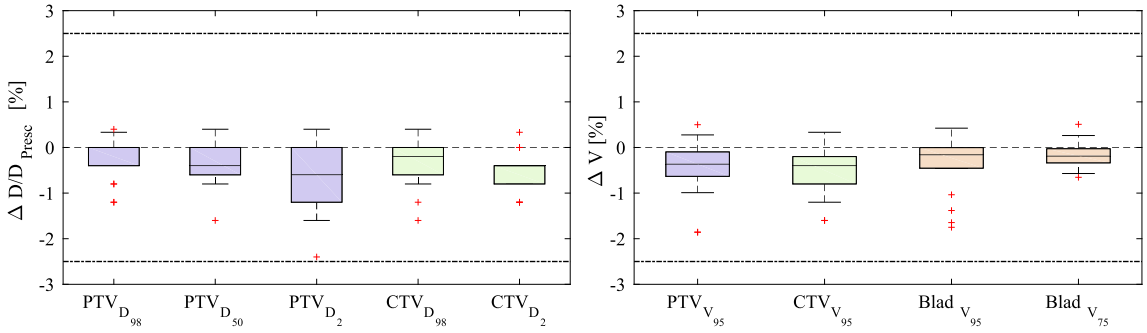

Fig. 2. Boxplots of targets (CTV in blue, PTV in green) and OARs (red) DVH parameter differences between CT and sCT (CT−sCT). The values are rescaled to the prescribed dose (left panel) or the total volume of the specific structure (right panel). The bar of the boxplot indicates the inter-quartile range and with outliers defined by a whisker of 1.5 the inter-quartile range.

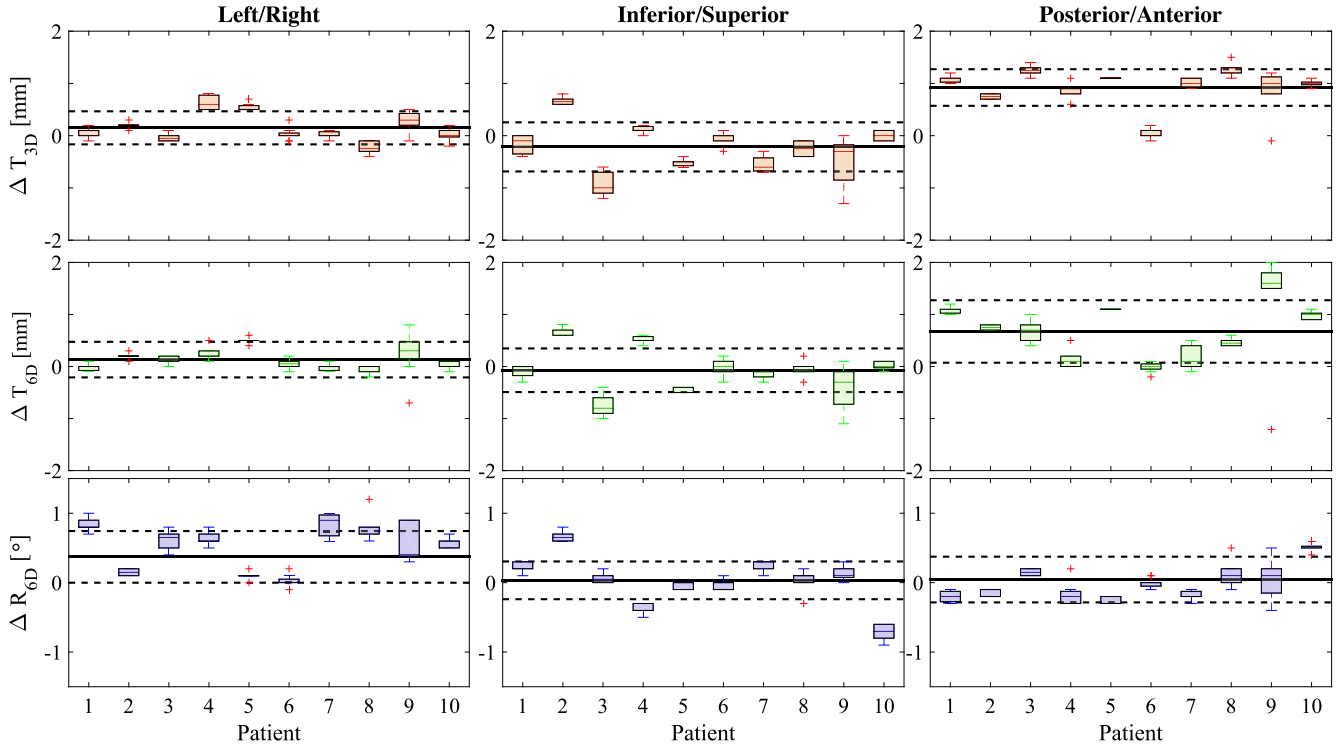

Fig. 3. Boxplots of the difference in translation (T, in mm, red and green for three and six DoF registrations, respectively) and rotation (R, in ◦, blue) between the set-up corrections obtained registering CBCT to sCT minus CBCT to CT_{reg} for ten patients in the left-right (left panels), inferior-superior (middle panel) and posterior-anterior (right panels) directions. In the case of the rotation, the direction indicates the rotation axis. The bar of the boxplot indicates the inter-quartile range and with outliers defined by a whisker of 1.5. The black continuous line indicates the average of mean difference over the patients, while the black dashed lines are positioned at a 95% confidence interval from the average mean over all the patients.

Table 3
Differences in automatic patient set-up corrections between sCT-based and standard CT-based registration. The statistics are reported for three and six degrees of freedom (DoF) registrations in the left-right (LR), inferior-superior (IS) and posterior-anterior (AP) directions. The values are expressed in mm for the translations and degrees for the rotations in terms of mean (± 1σ), and range [min; max]. Bold values represent the cases of nonequivalence, as statistical differences were found in the two one-sided tests.

Registrations	Dir	Translation [mm]		Rotation [°]	
		$\bar{x} \pm \sigma$	[min; max]	$\bar{x} \pm \sigma$	[min; max]
Bone six DoF	LR	0.1 ± 0.2	[−0.7;0.8]	0.5 ± 0.4	[−0.1;1.2]
T + R	IS	−0.1 ± 0.4	[−1.1;0.8]	0.0 ± 0.4	[−0.9;0.8]
Clipbox	PA	**0. 7 ± 0. 6**	[−1.2;2.0]	0.0 ± 0.3	[−0.4;0.6]
Bone three DoF	LR	0.1 ± 0.3	[−0.4;0.8]		
T	IS	−0.2 ± 0.4	[−1.3;0.8]		
Clipbox	PA	**0. 9 ± 0. 4**	[−0.1;1.5]		

this difference needs to be reviewed in the light of the total uncertainty accepted in radiation therapy [35]. It is important to bear in mind that the reported difference is within the voxel size of the MR images, and for registrations, the largest deviation was obtained with three DoF registration. For our clinic, this difference was not considered relevant as we only use six DoF registrations. However, the results highlight that sites should perform independent evaluations for systematic offsets before introducing MR-only into the clinic. To fully understand the cause of this deviations, further investigations into the origin of the systematic deviations will be performed prior to clinical introduction. In particular, we hypothesise that three factors may contribute to the deviations. The first factor related to the difference that may arise during simulations on CT and MR may differ, e.g. the position of immobilisation wedges may impact the inclination of the legs, or the flat table may be inclined in the MRI. Besides, physiological changes may occur. In this sense, it was reported that the anterior-posterior direction is the most prone to systematic motion [36]. Also, previous investigations already hypothesised that bladder and rectal filling may lead to different positions in the anterior-posterior directions [18,22]. The second factor relates to the sCT generation method. In this factor, we also include the geometric distortion that may compromise MRI and derived sCT images [37]. Finally, the third factor relates to sCT generation and CT to sCT registration: the analysis assumed that CT to sCT registration was perfect. In reality, residual error may still be present. In this study, we registered CT to sCT images over the entire body, while for position verification purposes, registration based on the bone match within the clipbox is considered to be clinically relevant. In addition, in our study, utilising different algorithms and software when aligning CT with sCT and when registering CBCT images may have contributed to the systematic differences observed.

To our knowledge, no other study investigated the impact of position verification for rectal cancer patients within an MR-only radiotherapy pathway. To enable a comparison with previous work, we compared our results with studies on prostate cancer patients, given the anatomical proximity. For example, Korhonen et al. [38] investigated the impact of sCT- and MR-based set-up corrections for position verification based both on CBCT and planar imaging. They obtained accuracy higher than 0.5 mm and precision higher than 1 mm, which is in line with our results. Doemer et al. found that CBCT-based position verification using MR as a reference did not impact the CTV-to-PTV margin recipe [39]. Also, they reported that the PA direction was affected by the largest differences in shift position due to non-compliance with bowel preparation at the MRI and CT simulations. The study conducted by Kemppainen et al. [40], who utilised the same commercial sCT generation solution, investigated the impact of position verification performed using digitally reconstructed radiography (DRR) for prostate cancer. Interestingly, they also reported a 0.5 mm systematic

difference in the anterior-posterior direction. This is in line with our findings, supporting the hypothesis that the systematic difference may be intrinsic to the sCT generation method or be caused by registration errors or inter-scan motion and was not related to patient simulation. This, however, requires further investigations that are currently undergoing.

Alternatively, MR images could be directly used as a reference for position verification. This may solve the deviations found in our study by eliminating the use of sCT for position verification. However, the software we used to perform set-up correction did not allow importation of MR images and support multi-modality image registration.

In general, it is essential to note that the assessment of the impact of sCT generation methods to total geometric accuracy is as critical as dosimetric accuracy [40]. Currently, assessments of dosimetric accuracy outnumber investigations of the impact of other areas of uncertainty in radiotherapy. This study contributed to evaluating the overall impact of a commercially available sCT generation method for an anatomical region that has not been largely investigated. Specifically, this work presented the first study investigating the impact of position verification for rectal cancer patients within an MR-only radiotherapy pathway.

In conclusion, this study shows that sCT images generated with the adopted commercial solution for prostate cancer radiotherapy are clinically acceptable for accurate dose calculations and position verification for rectal cancer radiotherapy. We reported that mean differences against CT-based dose calculations were within 0.5% and the use of sCT for position verification would impact CBCT registration less than 1 mm. A deviation of about 0.7 mm within the anterior-posterior was the largest concern for position verification, and future investigations will be performed to fully understand the underlying causes.

Acknowledgements

The research is partially funded by ZonMw IMDI Programme, project number: 1040030. The project is co-funded by Philips Healthcare. Jan J W Lagendijk and Max A Viergever offered general support to the research. The authors would like to thank Guus G Veenendaal for the help provided with XVI and CBCT registrations.

Conflict of interest statement

Rob Tijssen and Cornelis A T van den Berg declare to be a minority shareholder of MRCode BV. Peter R Seevinck claims to be a shareholder of MRIGuidance BV.

Appendix A. Supplementary data

Supplementary data associated with this article can be found, in the online version, at https://doi.org/10.1016/j.phro.2018.09.002.

References

[1] Kye BH, Cho HM. Overview of radiation therapy for treating rectal cancer. Ann Coloproct 2014;30:165–74. https://doi.org/10.3393/ac.2014.30.4.165.
[2] van de Velde CJ, Boelens PG, Borras JM, Coebergh JW, Cervantes A, Blomqvist L, et al. EURECCA colorectal: multidisciplinary management: European consensus conference colon & rectum. Europ J Canc 2014;50:1.e1–1.e34. https://doi.org/10.1016/J.EJCA.2013.06.048.
[3] van Gijn W, Marijnen CA, Nagtegaal ID, Kranenbarg EMK, Putter H, Wiggers T, et al. Preoperative radiotherapy combined with total mesorectal excision for resectable rectal cancer: 12-year follow-up of the multicentre, randomised controlled TME trial. Lancet Oncol 2011;12:575–82. https://doi.org/10.1016/S1470-2045(11)70097-3.
[4] Dirix P, Haustermans K, Vandecaveye V. The value of magnetic resonance imaging for radiotherapy planning. Semin Radiat Oncol 2014;24:151–9.
[5] Taylor FG, Quirke P, Heald RJ, Moran B, Blomqvist L, Swift I, et al. Preoperative high-resolution magnetic resonance imaging can identify good prognosis stage I, II, and III rectal cancer best managed by surgery alone: a prospective, multicenter, European Study. Ann Surg 2011;253:711–9. https://doi.org/10.1097/sla.0b013e31820b8d52.
[6] Shihab OC, Moran BJ, Heald RJ, Quirke P, Brown G. MRI staging of low rectal cancer. Eur Radiol 2009;19:643–50. https://doi.org/10.1007/s00330-008-1184-6.
[7] Tan J, Lim Joon D, Fitt G, Wada M, Lim Joon M, Mercuri A, et al. The utility of multimodality imaging with CT and MRI in defining rectal tumour volumes for radiotherapy treatment planning: a pilot study. J Med Imag Radiat Oncol 2010;54:562–8. https://doi.org/10.1111/j.1754-9485.2010.02212.x.
[8] Gwynne S, Webster R, Adams R, Mukherjee S, Coles B, Staffurth J. Image-guided radiotherapy for rectal cancer – a systematic review. Clin Oncol 2012;24(4):250–60. https://doi.org/10.1016/j.clon.2011.07.012.
[9] Brown RW, Cheng YCN, Haacke EM, Thompson MR, Venkatesan R. Magnetic Resonance Imaging: Physical Properties and Sequence Design. Wiley0471720852; 2014.
[10] Schmidt MA, Payne GS. Radiotherapy planning using MRI. Phys Med Biol 2015;60:R323–61. https://doi.org/10.1088/0031-9155/60/22/R323.
[11] Fraass BA, McShan DL, Diaz RF, Ten Haken RK, Aisen A, Gebarski S, et al. Integration of magnetic resonance imaging into radiation therapy treatment planning: I. Technical considerations. Int J Radiat Oncol Biol Phys 1987;13:1897–908. https://doi.org/10.1016/0360-3016(87)90358-0.
[12] Lee YK, Bollet M, Charles-Edwards G, Flower MA, Leach MO, McNair H, et al. Radiotherapy treatment planning of prostate cancer using magnetic resonance imaging alone. Radiother Oncol 2003;66:203–16. https://doi.org/10.1016/S0167-8140(02)00440-1.
[13] Devic S. MRI simulation for radiotherapy treatment planning. Med Phys 2012;39:6701. https://doi.org/10.1118/1.4758068.
[14] Karlsson M, Karlsson MG, Nyholm T, Amies C, Zackrisson B. Dedicated magnetic resonance imaging in the radiotherapy clinic. Int J Radiat Oncol Biol Phys 2009;74:644–51. https://doi.org/10.1016/j.ijrobp.2009.01.065.
[15] Edmund JM, Nyholm T. A review of substitute CT generation for MRI-only radiation therapy. Radiat Oncol 2017;12:28. https://doi.org/10.1186/s13014-016-0747-y.
[16] Johnstone E, Wyatt JJ, Henry AM, Short SC, Sebag-Montefiore D, Murray L, et al. A systematic review of synthetic CT generation methodologies for use in MRI-only radiotherapy. Int J Radiat Oncol Biol Phys 2017:100. https://doi.org/10.1016/J.IJROBP.2017.08.043.
[17] Owrangi AM, Greer PB, Glide-Hurst CK. MRI-only treatment planning: benefits and challenges. Phys Med Biol 2018:63. https://doi.org/10.1088/1361-6560/aaaca4.
[18] Persson E, Gustafsson C, Nordström F, Sohlin M, Gunnlaugsson A, Petruson K, et al. MR-OPERA – a Multi-center/multi-vendor validation of MRI-only prostate treatment planning using synthetic CT images. Int J Radiat Oncol Biol Phys 2017;99:692–700. https://doi.org/10.1016/j.ijrobp.2017.06.006.
[19] Maspero M, Seevinck PR, Schubert G, Hoesl MAU, van Asselen B, Viergever MA, et al. Quantification of confounding factors in MRI-based dose calculations as applied to prostate IMRT. Phys Med Biol 2017;62:948–65. https://doi.org/10.1088/1361-6560/AA4FE7.
[20] Tyagi N, Fontenla S, Zhang J, Cloutier M, Kadbi M, Mechalakos J, et al. Dosimetric and workflow evaluation of first commercial synthetic CT software for clinical use in pelvis. Phys Med Biol 2017;62:2961–75. https://doi.org/10.1088/1361-6560/aa5452.
[21] Kemppainen R, Suilamo S, Tuokkola T, Lindholm P, Deppe MH, Keyriläinen J. Magnetic resonance-only simulation and dose calculation in external beam radiation therapy: a feasibility study for pelvic cancers. Acta Oncol 2017;56:792–8. https://doi.org/10.1080/0284186X.2017.1293290.
[22] Wang H, Du K, Qu J, Chandarana H, Das IJ. Dosimetric evaluation of magnetic resonance-generated synthetic CT for radiation treatment of rectal cancer. PLoS ONE 2018;13:e0190883. https://doi.org/10.1371/journal.pone.0190883.
[23] Dixon WT. Simple proton spectroscopic imaging. Radiology 1984;153:189–94.
[24] Eggers H, Brendel B, Duijndam A, Herigault G. Dual-echo Dixon imaging with flexible choice of echo times. Magn Reson Med 2011;65:96–107. https://doi.org/10.1002/mrm.22578.
[25] Burbach J, Kleijnen J, Reerink O, Seravalli E, Me P, Schakel T, et al. Inter-observer agreement of MRI-based tumor delineation for preoperative radiotherapy boost in locally advanced rectal cancer. Radiother Oncol 2016;118:399–407. https://doi.org/10.1016/J.RADONC.2015.10.030.
[26] Bol GH, Kotte ANTJ, Lagendijk JJW. Volumetool: an image evaluation, registration, and delineation system for radiotherapy. Phys Med 2003;19:80.
[27] de Boer HC, Heijmen BJ. eNAL: an extension of the NAL setup correction protocol for effective use of weekly follow-up measurements. Int J Radiat Oncol Biol Phys 2007;67:1586–95. https://doi.org/10.1016/J.IJROBP.2006.11.050.
[28] van Herk M, de Munck JC, Lebesque JV, Muller S, Rasch C, Touw A. Automatic registration of pelvic computed tomography data and magnetic resonance scans including a full circle method for quantitative accuracy evaluation. Med Phys 1998;25:2054–67. https://doi.org/10.1118/1.598393.
[29] Low DA. Gamma dose distribution evaluation tool. J Phys 2010;250:012071. https://doi.org/10.1088/1742-6596/250/1/012071.
[30] Schuirmann DJ. A comparison of the two one-sided tests procedure and the power approach for assessing the equivalence of average bioavailability. J Pharmac Biopharm 1987;15:657–80. https://doi.org/10.1007/BF01068419.
[31] Liu L, Jolly S, Cao Y, Vineberg K, Fessler JA, Balter JM. Female pelvic synthetic CT generation based on joint intensity and shape analysis. Phys Med Biol 2017;62:2935–49. https://doi.org/10.1088/1361-6560/62/8/2935.
[32] ICRP. International Commission on Radiation Protection: Prevention of Accidents to Patients Undergoing Radiation Therapy. Elsevier Health Sciences; 2000. vol. 86.
[33] Thwaites D. Accuracy required and achievable in radiotherapy dosimetry: have modern technology and techniques changed our views? J Phys 2013;444:012006. https://doi.org/10.1088/1742-6596/444/1/012006.
[34] Verellen D, Ridder MD, Linthout N, Tournel K, Soete G, Storme G. Innovations in image-guided radiotherapy. Nat Rev Cancer 2007;7:949–60. https://doi.org/10.

1038/nrc2288.
[35] van der Merwe D, Van Dyk J, Healy B, Zubizarreta E, Izewska J, Mijnheer B, et al. Accuracy requirements and uncertainties in radiotherapy: a report of the International Atomic Energy Agency. Acta Oncol 2017;56:1–6. https://doi.org/10.1080/0284186X.2016.1246801.
[36] Scaife J, Harrison K, Romanchikova M, Parker A, Sutcliffe M, Bond S, et al. Random variation in rectal position during radiotherapy for prostate cancer is two to three times greater than that predicted from prostate motion. Brit J Radiol 2014;87:20140343. https://doi.org/10.1259/bjr.20140343.
[37] Jezzard P. Physical basis of spatial distortions in magnetic resonance images. In: Bankman IN, editor. Handbook of Medical Imaging. Orlando, FL, USA: Academic Press, Inc.; 2000. p. 425–38. ISBN 0-12-077790-8.
[38] Korhonen J, Kapanen M, Sonke JJ, Wee L, Salli E, Keyriläinen J, et al. Feasibility of MRI-based reference images for image-guided radiotherapy of the pelvis with either cone-beam computed tomography or planar localization images. Acta Oncol 2015;54:889–95. https://doi.org/10.3109/0284186X.2014.958197.
[39] Doemer A, Chetty IJ, Glide-Hurst C, Nurushev T, Hearshen D, Pantelic M, et al. Evaluating organ delineation, dose calculation and daily localization in an open-MRI simulation workflow for prostate cancer patients. Radiat Oncol 2015;10:37. https://doi.org/10.1186/s13014-014-0309-0.
[40] Kemppainen R, Vaara T, Joensuu T, Kiljunen T. Accuracy and precision of patient positioning for pelvic MR-only radiation therapy using digitally reconstructed radiographs. Phys Med Biol 2018;63:055009. https://doi.org/10.1088/1361-6560/aaad21.